Simulating the motion of the leech: A biomechanical application of DAEs

Wolf–Jürgen Beyn*
email: beyn@mathematik.uni-bielefeld.de

Christian Alscher *†
email: alscher@mathematik.uni-bielefeld.de

Department of Mathematics, University of Bielefeld
Postfach 100131, D–33501 Bielefeld, Germany

Abstract

In this paper a mathematical model is developed for the dynamical behaviour of a hydrostatic skeleton. The basic configuration is taken from the worm–like shape of the medicinal leech. It consists of a sequence of hexahedra with damped elastic springs as edges to model the various parts of the musculature. The system is stabilized by the constraint of constant volume either in the whole body or in prescribed compartments. We set up Lagrange's equations of motion with the Lagrange multipliers being the pressure values in the compartments. The equations of motion lead to a large differential–algebraic system which is solved by an application of semi–explicit numerical methods. Though the model has not yet been adapted to experimental data, first simulations with a simplified set of parameters show that it is capable of generating basic movements of the leech such as crawling and swimming.

Keywords: Lagrange's equations of motion, viscoelasticity, semi–explicit methods

AMS subject classification: 92C10

*supported by DFG Schwerpunktprogramm "Ergodentheorie, Analysis und effiziente Simulation dynamischer Systeme".

†supported by DFG Graduiertenkolleg "Strukturbildungsprozesse", FSP Mathematisierung, University of Bielefeld, Germany

1 Introduction

The constructional principle of the *hydrostatic skeleton* can be found in many worm–like animals [17]. Even reptilian tongues [3] and the trunk of an elephant [9] are built up according to this constructional principle.
In physical terms the hydrostatic skeleton is realized as an *incompressible fluid* enclosed by an *elastic body wall*. Contraction or relaxation of muscles embedded in the body wall leads to changes in the shape of the body. The functional principles of the hydrostatic skeleton are not easily understood on a purely intuitive basis [2], since the contraction of a single muscle affects, in principle, the shape of the whole body.
In order to get an integrative insight in the complex functional principles, a simulation–based approach was chosen in [20]. The known physical principles were combined into a mathematical model, which can be used to study equilibrium states of the hydrostatic skeleton for a given volume and for prescribed activations of the muscles. The biomechanical model was based on a particular animal, the *medicinal leech*. Its behaviour and physiological structure has been extensively studied [10],[15], and the neuronal control and properties of the muscles are well understood [13],[14],[18]. In [20], [21] and [22] several quasi–static features were studied using this model, e.g. deformations and pressure variations caused by activation of groups of muscles. In [16] an extended steady state model was developed to incorporate a refined geometry as well as experimental data on muscle behaviour.
In this paper we introduce a dynamical model in order to study the mechanical properties of the body during fast motions such as crawling and swimming. Muscles will be modelled as damped elastic springs and the volume constraints will be kept. The equations of motion lead to a system of differential–algebraic equations which will be solved numerically in case of a crawling sequence and a swimming cycle. For the solution we used the code MEXX [12] and took advantage of the sparsity patterns of the matrices that occur in our application.

2 The medicinal leech

The anatomy of the medicinal leech *(Hirudo medicinalis L.)* is quite complex; a sketch of the cross–section of its body can be found in [14],[18]. The cylindrical body consists of 21 segments and there are two suckers at front and rear ends of the animal. Three different muscle layers that lie below the cuticle constitute the longitudinal, the oblique and the circular musculature of the leech. In addition, dorsoventral muscles pass through the body from the dorsal to the ventral body wall. Fig.1 shows a characteristic length–tension relation of the longitudinal musculature in the passive and the active state.

Leeches move either by crawling or swimming; detailed kinematic studies of these motions can be found in [10],[15]. In the first phase of the crawling sequence the front sucker is released and

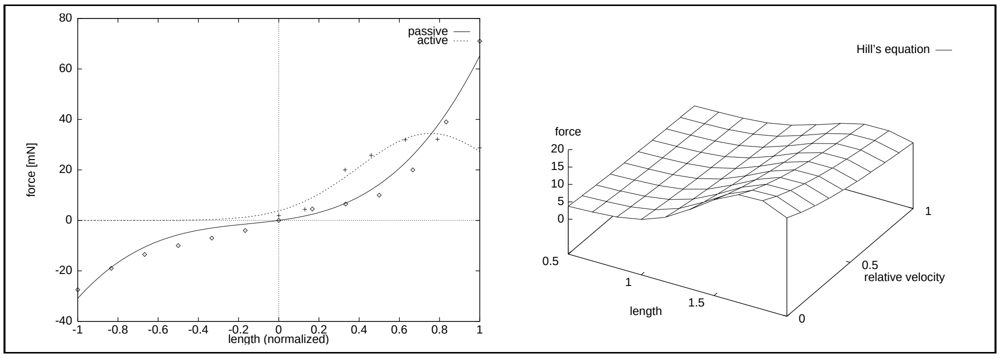

Figure 1: Left diagram: Active (upper curve) and passive (lower curve) length–tension relation of the longitudinal muscle of the leech. A 3rd order polynomial was fitted to passive experimental data from [18] and a Gaussian distribution function to unpublished active data (L–Cell stimulation) from Wilson. The value -1 corresponds to the minimal, 0 to the anesthetized and 1 to the maximal length of the muscle. Notice that the longitudinal muscle of an intact animal can produce a force of up to 600mN, so the diagram shows the active length–tension relation only qualitatively. Right diagram: Force exerted by a single elastic element at different lengths and relative velocities in the nonlinear case.

the body elongates by activation of the circular and relaxation of the longitudinal muscles. After the attachment of the front sucker the rear sucker is released and the body shortens by activation of the longitudinal and relaxation of the circular muscles. The sequence of swimming is realized by a wavy activation of the ventral longitudinal muscles, while the dorsal longitudinal muscles are activated with a phase shift. Throughout the movement the body is flattened by activation of the dorsoventral muscles.

Our intention is not to develop a dynamical model fully adapted to these experimental data. This is a considerable task even for the stationary case, see [16], [21] and [22]. Rather our intention is to develop a simple model which is sufficiently general to incorporate specific experimental data later on.

3 The dynamical model

The model consists of N connected hexahedral segments with $n = 4N + 4$ corners, *elastic edges* and *constant total volume*, see Fig.2. The shape of the model at time t is determined by the coordinate vector $q(t) = (q_1(t), \ldots, q_n(t))^T$, $q_i(t) \in \mathbb{R}^3$, $i = 1 \ldots n$ of the corners. The vector of velocities is given by $u(t) = \dot{q}(t) \in \mathbb{R}^{3n}$ and we assume the total mass to be distributed over the whole body with masses $m_i > 0$, $i = 1 \ldots n$ in the corners.

3.1 The elastic edges

The longitudinal and circular musculature of the hydrostatic skeleton of the leech is represented by the longitudinal and circular elastic elements in our model (LEs and CEs), while the dorsoventral muscles are included as part of the lateral CEs. Oblique muscles are neglected at present.
We assume that every elastic edge acts as a combination of a spring and a dashpot arranged in parallel. This mechanical model, called a *Voigt body*, is used to simulate the *viscoelastic* behaviour of the leech muscles (for more details see [6]).
As a first approximation of the nonlinear length–tension relation shown in Fig.1 we use the linear *Hooke's Law* combined with a linear dashpot. Consider first a single elastic element between two adjacent corners $q_i, q_j \in \mathbb{R}^3$ with velocities $u_i, u_j \in \mathbb{R}^3$ for $i \neq j$ and $1 \leq i, j \leq n$. At time t the force exerted at q_i by this elastic element is of the form

$$f_{ij}(t,q,u) := (\underbrace{E_{ij}(q_i,q_j)}_{\text{elasticity}} - \underbrace{d_{ij} D_{ij}(q_i,q_j,u_i,u_j)}_{\text{damping}}) \underbrace{\frac{(q_j - q_i)}{\|q_j - q_i\|_2}}_{\text{direction of force}}$$

with the elastic and damping terms given by

$$E_{ij}(q_i,q_j) = a_{ij}(t)(\underbrace{\|q_j - q_i\|_2}_{\text{distance}} - L_{ij}^{min}), \ D_{ij}(q_i,q_j,u_i,u_j) = \underbrace{(u_i - u_j)^T}_{\text{rel.velocity}} \frac{(q_j - q_i)}{\|q_j - q_i\|_2}. \qquad (1)$$

Here $\|q_j - q_i\|_2$ denotes the Euclidean distance of the points q_i and q_j. For every single elastic element the minimal length L_{ij}^{min}, the activation $a_{ij}(t)$ at time t and the damping parameter d_{ij} are to be prescribed.
So far only the elastic and damping properties in the direction of the muscles are incorporated into the model. Shear forces are not yet taken into account and we are not aware of any experimental data of this type. But nonlinear length–tension relations of the muscles can be built into the model by an appropriate choice of the functions E_{ij}. *Hill's equation* gives a reasonable approximation of the force–length–velocity relation of the muscles at fixed lengths (see [6], ch.9.7). It expresses the tension P of a contracting muscle in terms of the velocity v and the maximum tension P_0 at the fixed initial length L

$$P(L,v) = \frac{bP_0(L) - va}{v + b}, \quad \text{where } a \text{ and } b \text{ are constants.}$$

Setting $a = b = 1$ and using for $P_0(L)$ the nonlinear curve from Fig.6 (right diagram) we obtain the force–length–velocity relation shown in Fig.1 (right diagram).
If the muscle is in general position we use Hill's equation with $b = 1$, relative velocity $v = D_{ij}$ and damping parameter $a = d_{ij}$. Combining this with a length–tension relation obtained from the steady state case leads to the expression

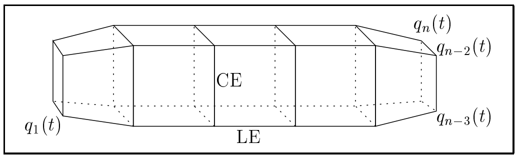

Figure 2: Sketch of an uncompartmentalized model with $N = 5$ segments and $n = 24$ corners.

$$f_{ij}(t,q,u) := \left(\frac{E_{ij}(q_i,q_j) - d_{ij} D_{ij}(q_i,q_j,u_i,u_j)}{D_{ij}(q_i,q_j,u_i,u_j)+1} \right) \frac{(q_j - q_i)}{\|q_j - q_i\|_2},$$

$$\text{where} \quad E_{ij}(q_i,q_j) = a_{ij}(t) E^a_{ij}(\|q_j - q_i\|_2) + E^p_{ij}(\|q_j - q_i\|_2).$$

The function E^a_{ij} has the shape of the active and E^p_{ij} the shape of the passive length–tension curve shown in Fig.1 (left diagram). The activation parameter $a_{ij}(t)$ takes values between 0 and 1 and it controls the level of activation of the elastic edge.
Depending on the position there are 3 or 4 elastic elements acting on each corner (see Fig.2), so the total force acting on q_i at time t results to

$$F_i(t,q,u) := \sum_{j \in I(i)} f_{ij}(t,q,u), \tag{2}$$

where the set $I(i) \subset \{1 \dots n\}$ contains the indices of the corners adjacent to q_i.

3.2 The constraint of constant volume

The model is based on the assumption that the total volume, which is the sum of the volumes of all segments, remains constant during the movement. In order to prevent volume exchanges adjacent segments can also be grouped into compartments, so in a model with m compartments we find the constraints

$$\sum_{j=\alpha_k}^{\beta_k} V_j(q(t)) = V_k^{tot}, \quad k = 1 \dots m, \tag{3}$$

where V_k^{tot} is the prescribed volume of the kth compartment, and $V_j(q(t))$ expresses the volume of the jth segment in terms of the coordinate vector $q(t)$. Appropriate formulas for these functions can be found in [20] where the hexahedral elements are taken as trilinear images of the unit cube. In (3) α_k and β_k denote the numbers of the first and the last segment in the kth compartment.
In order to simulate the food intake of the leech we allow the volumes of the compartments to vary in time. So in general we find the constraints

$$g_k(t,q(t)) = 0, \quad k = 1 \dots m, \quad \text{where} \quad g_k(t,q) := \sum_{j=\alpha_k}^{\beta_k} V_j(q) - V_k^{tot}(t). \tag{4}$$

Here $V_k^{tot}(t)$ is the prescribed volume of the kth compartment at time t. Notice that the volume exchanges are assumed to be frictionless, therefore the constraints in (4) are *holonomic.*

3.3 The equations of motion

The motion of the model is described by the coordinates $q(t)$ and velocities $u(t) = \dot{q}(t)$ of the corners and the pressures in the compartments. We determine these unknowns by solving *Lagrange's equations of motion* with *holonomic constraints*

$$\begin{aligned} m_i \ddot{q}_i(t) &= F_i(t, q(t), u(t)) - \sum_{k=1}^{m} \lambda_k(t) \frac{\partial g_k}{\partial q_i}(t, q(t)), \quad i = 1 \dots n \\ 0 &= g_k(t, q(t)), \quad k = 1 \dots m\,. \end{aligned}$$

Here the total force acting on the corner q_i results from the *inner force* (2) which is exerted by the elastic elements and the *force of constraint* which arises from the volume constraints (4), see e.g. [7]. The *Lagrange multiplier* $\lambda_k(t)$ corresponds to the pressure in the kth compartment at time t and the m_i are assumed to be lumped masses concentrated near the corners q_i. We have not incorporated the fact that these masses might change with time if considerable variations in the segmental volumes occur. Introducing the vectors

$$F(t, q, u) := (F_1(t, q, u), \dots, F_n(t, q, u))^T, \quad g(t, q) := (g_1(t, q), \dots, g_m(t, q))^T$$

and the matrices

$$G(t, q) := \frac{\partial g}{\partial q}(t, q), \quad M := \mathrm{diag}(m_1, m_1, m_1, \dots, m_n, m_n, m_n)$$

we arrive at a first order DAE–system

$$\begin{aligned} \dot{q}(t) &= u(t) && (5) \\ M\dot{u}(t) &= F(t, q(t), u(t)) - G(t, q(t))^T \lambda(t) && (6) \\ 0 &= g(t, q(t)) && (7) \end{aligned}$$

of index 3, where $\lambda(t) := (\lambda_1(t), \dots, \lambda_m(t))^T$. Even though the model is geometrically simplified the system (5)–(7) contains $3n+3n+m = 549$ unknowns when a fully compartmentalized model ($m = N$) with $N = 21$ segments is used (see simulations below).

We use the numerical methods from [12] (code MEXX) which turned out to be quite efficient for this type of equations. In a first step the algebraic constraint (7) is replaced by its time derivative in order to reduce the index of the DAE–system from 3 to 2 (descriptor form). A modification of the *semi–explicit Euler method* yields the scheme

$$\begin{aligned} q^{j+1} &= q^j + hu^j && (8) \\ Mu^{j+1} &= Mu^j + hf(t^j, q^j, u^j) - hG(t^{j+1}, q^{j+1})^T \lambda^{j+1} && (9) \\ 0 &= g_t(t^{j+1}, q^{j+1}) + G(t^{j+1}, q^{j+1}) u^{j+1} && (10) \end{aligned}$$

for $j = 0 \dots w-1$ with step size $h := t^*/w$, $w \in \mathbb{N}$ on the time interval $[0, t^*]$. Consistent initial values $q^0 \in \mathbb{R}^{3n}$, $u^0 \in \mathbb{R}^{3n}$, $\lambda^0 \in \mathbb{R}^m$ satisfying $g(0, q^0) = 0$ and $g_t(0, q^0) + G(0, q^0)u^0 = 0$ are required. The semi–explicit form of the method avoids solving a large nonlinear system. Rather, q^{j+1} is determined directly from (8) and we are left with the symmetric linear system

$$\begin{pmatrix} M & G(t^{j+1}, q^{j+1})^T \\ G(t^{j+1}, q^{j+1}) & 0 \end{pmatrix} \begin{pmatrix} u^{j+1} \\ h\lambda^{j+1} \end{pmatrix} = \begin{pmatrix} Mu^j + hf(t^j, q^j, u^j) \\ -g_t(t^{j+1}, q^{j+1}) \end{pmatrix}. \tag{11}$$

In addition, after each time step q^{j+1} is projected orthogonally onto the manifold defined by (7). The nonlinear system arising in the projection step is solved by a simplified Newton iteration which requires the solution of linear systems with a matrix of the block structure in equation (11). The implementation includes an extrapolation method with order and step size control, and the sparsity pattern of the above matrix, i.e. the diagonal mass matrix M and the banded structure of the Jacobian G is taken into account. Furthermore a dense output of the solution is used to visualize the solution. More details can be found in [1]; a video–tape with some simulations can be obtained from the authors [1].

4 Simulations

In this section we present the simulation of the two most important behaviours of the leech, namely crawling and swimming. Furthermore we study the influence of damping and nonlinear length–tension relations of the elastic edges on the motion of our model.

At the beginning of all simulations the model is in the so–called *resting state*. In this equilibrium state we choose the parameters to resemble the shape of the leech in the anaesthetized state.

The body of the leech is not compartmentalized, but volume exchanges between adjacent segments are rarely observed in experiments. Therefore we chose a fully compartmentalized model with $N = 21$ segments, except for the sequence of crawling, where 3 segments at the front and the rear end of the model are grouped to compartments in order to simulate the suckers of the leech. The total volume of each compartment is fixed at $V_k^{tot} = 1$, $k = 1 \dots m$ and the masses in the corners are set to $m_i = 0.001$, $i = 1 \dots n$. For every single elastic element between two adjacent corners $q_i, q_j \in \mathbb{R}^3$ for $i \neq j$ and $1 \leq i, j \leq n$ we chose the minimal length $L_{ij}^{min} = 0.5$, the resting activation $a_{ij}(t) = 1$ at time $t \in [0, t^*]$ and the damping factor $d_{ij} = 0.1$. In the following simulations the elastic elements are at resting activation unless stated otherwise.

Notice that these values do not yet correspond to experimental data of the leech. An adaptation of the static model is in preparation (see [21],[22]), which includes a geometric adaptation and realistic nonlinear length–tension relations of the elastic elements (see Fig.1), compare

[1] see also http://www.mathematik.uni-bielefeld.de/˜alscher

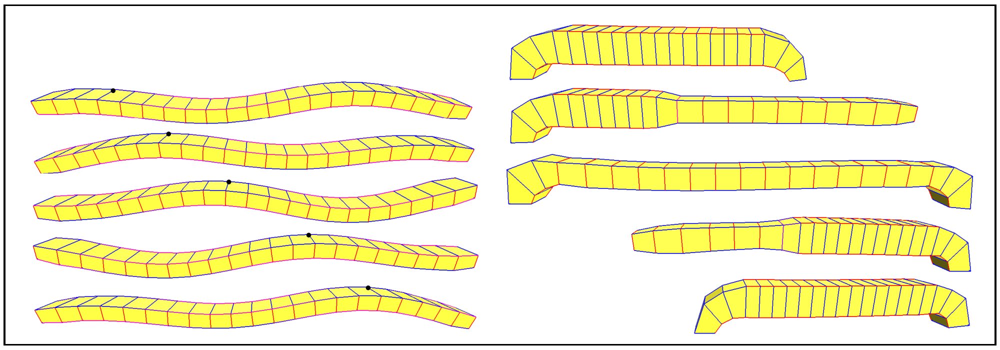

Figure 3: Left: Simulation of the sequence of swimming. Right: Simulation of the sequence of crawling. Notice that the first 3 and the last 3 segments are grouped to compartments.

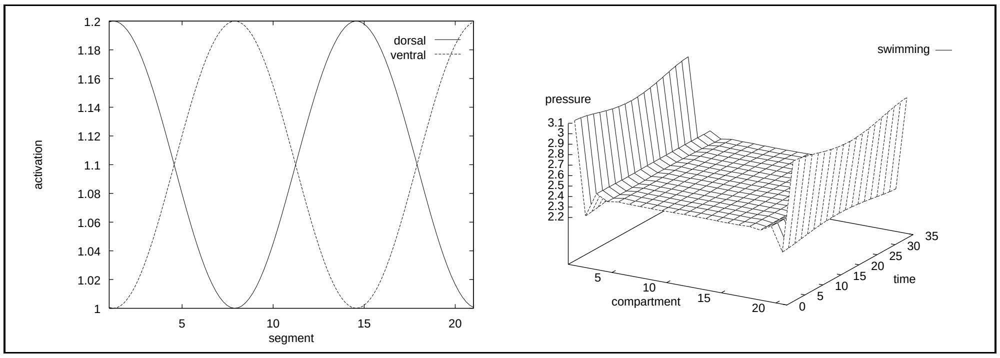

Figure 4: Activation pattern of the LEs (ventral and dorsal) in the intermediate state $t = 17$ of the swimming cycle (left diagram) and pressure distribution in the $m = 21$ compartments during the sequence of swimming (right diagram).

also [16]. For the dynamical model there is still a considerable lack of experimental data in order to set up a realistic force function (2).

The simulation of the *sequence of swimming* in the time interval $[0, 35]$ is shown in Fig.3. The dorsoventral muscles of the leech are simulated by the lateral CEs in our model, so we chose a high level of activation of the lateral CEs ($a_{ij}(t) = 6$) which flattens the body during the whole movement. The wavy activation pattern of the LEs is shown in Fig.4. The pressure in all compartments remains almost constant during the whole simulation (see Fig.4), but at the front and the rear end of the model the pressure is much higher than in the medial body region. Pressure fluctuations at the ends of the model are also observed in the steady–state simulations in [16]. We are not aware of any experiments supporting this observation; pressure measurements are usually made in medial segments (see [19]). Fig.3 also shows the shape of the model in different intermediate states of the simulation of the *crawling sequence*, which was already described in section 2. After the front sucker is released and lifted in the interval $[0, 5]$ the body elongates in the interval $[5, 20]$ by relaxation of the LEs and delayed

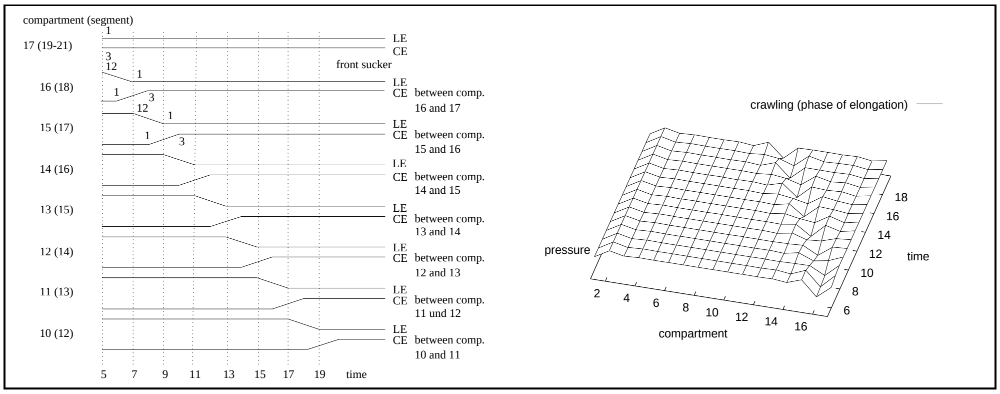

Figure 5: Left diagram: Activation pattern in the elongation phase ($t \in [5, 20]$) of the sequence of crawling. The small numbers in the diagram indicate the level of activation of the elastic elements. Right diagram: Pressure distribution in the $m = 17$ compartments during the elongation phase ($t \in [5, 20]$) of the crawling sequence.

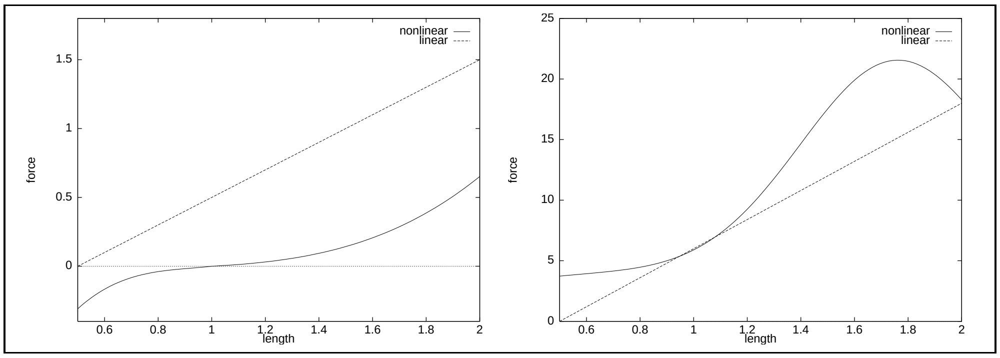

Figure 6: Scaling of the passive (left diagram) and active (right diagram) nonlinear length–tension curves (see Fig.1, left diagram). In the linear case we chose a minimal length of 0.5 and in equation (1) the activation parameters 1 (passive) and 12 (active) in order to make possible a sufficient elongation of the body (see Fig.3). In the nonlinear case we transformed the length intervals [-1,0] and [0,1] from Fig.1 (left diagram) linearly to [0.5,1] and [1,2], respectively. The passive curve from Fig.1 was multiplied by the factor 0.01 and the active curve was multiplied by 0.5; finally an offset of value 4 was added to the active curve.

In the simulations this enables the active muscles (agonists) to exert high forces at small lengths with weakly counteracting passive muscles (antagonists). Such an arrangement turned out to be necessary for the body to reach elongations comparable to experiments (see adaptations in [21],[22]).

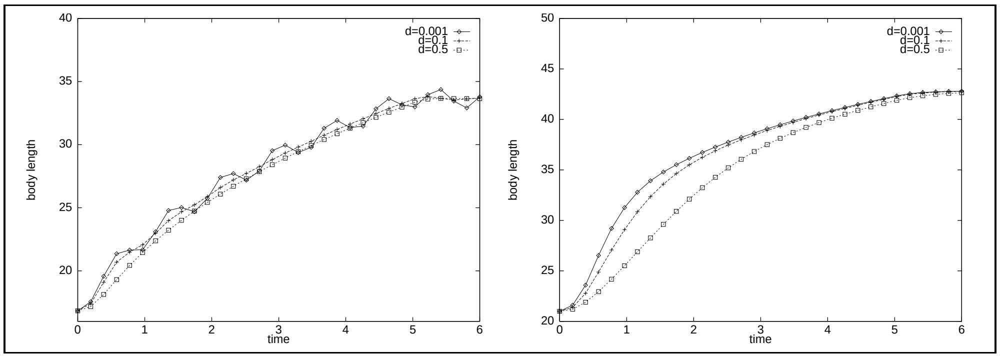

Figure 7: Body length plotted against time in the linear (left diagram) and in the nonlinear case (right diagram) using different damping parameters. The activation of all CEs is increased linearly in the time interval [0,5] from 1 to 8 (linear case) and from 0 to 1 (nonlinear case) and is then held fixed in the interval [5,6]. Throughout the simulation the activation of all LEs remains at resting level.

activation of the CEs, for details on the activation pattern see Fig.5. In simulations without the delay in activation the body starts to bulge between adjacent segments with different activation and the motion is not as smooth as in the simulation with the delay. Notice the pressure wave passing through the body and running in phase with the relaxation/activation wave of LEs and CEs (see Fig.5).

Activation of all CEs leads to an elongation of the body, a simple simulation that can be used to study the influence of damping and nonlinear length–tension relations (see Fig.1). In order to make a comparison of simulations with linear and nonlinear length–tension relations of the elastic edges possible we scaled the nonlinear curves, see Fig.6. Notice that in this scaling the passive linear curves do not have a vanishing force at resting length. Such modifications will be investigated after a more systematic adaptation in [21],[22]. Using the linear and nonlinear length–tension curves from Fig.6 we made the following simulations:
In the linear case the activation parameters of all CEs are increased linearly from 1 to 8 in the time interval $[0,5]$ and then held constant for $t \in [5,6]$, while the activation of the LEs remains at resting level. Fig.7 shows that the body length is doubled and that an increase of the damping leads to a much smoother simulation. In fact, the elastic edges are overdamped for $d = 0.5$ and nonoverdamped for $d = 0.001$ throughout the simulation, while they change type for the intermediate value $d = 0.1$.
In the nonlinear case we did the same simulation as above, except that we increased the activation parameters of the CEs linearly from 0 to 1. Fig.7 shows that the body length is also doubled, but the influence of damping on the smoothness of the motion is not as pronounced as in the linear case. The body length grows rapidly for $t \in [0,2]$, but saturates in the remaining time interval $[2,6]$. This effect can be explained by the very low passive forces of the LEs near the resting length, see Fig.6. Once the lengths reach the steep regions of these curves the elongation process slows down considerably.

The resting state in the nonlinear case consists of 21 equal cubes, since the force exerted by the passive elastic elements at resting length is equal to zero (see Fig.6). In the linear case the force at resting length is not equal to zero, the elastic edges start to shorten and the stabilization by the inner pressure leads to a body shape which is tapered at both ends.

5 Discussion

There is a collection of related work on the simulation of animal locomotion. In [5] fish swimming is studied using a 2–dimensional model which consists of a thread–like collection of moving mass points. The fluid quantities are represented on a square grid and the major aim of their model is to study the interaction of the body with the surrounding fluid and the fluid motion itself. The interaction forces are also incorporated in a model of the lamprey presented in [4]. This 2–dimensional model consists of a rigid skeleton, and a simulated neuronal oscillator is used to activate muscles which act on the links in order to control the bending of the body. More realistic physiological muscle properties of the leech are incorporated in a similar model introduced in [8]. This model can be used to study dynamical aspects of the leech during swimming, but the hydrostatic principle is not included. A more realistic biomechanical model of the hydrostatic skeleton of the leech can be found in [16]. The cross–section of that model is piecewise elliptical and it is already adapted to experimental data of the leech, but so far it is restricted to equilibrium states.
The dynamical model presented in this paper is an extension of an equilibrium model introduced in [20]. That model was used to study quasi–static behaviours of the leech, which are not affected by dynamical features of the body. The equilibrium model as well as the dynamical model presented here consists of a sequence of connected hexahedral segments with elastic edges and with the total volume assumed to be constant. These properties constitute the main features of the hydrostatic skeleton, so the model reflects the major properties of the constructional principle of the leech. It has not yet been adapted to experimental data and its geometrical shape is simplified considerably compared to the rounded body of the leech. We also did not include the forces exerted by the surrounding water on the body during swimming. Nevertheless the simulations with the approximate set of parameters show that our model suffices to study fast movements of the leech like swimming and crawling.

Acknowledgements

We thank W.B. Kristan Jr. (San Diego) for suggestions of activation patterns and R.J.A. Wilson (San Diego) for sharing experimental data underlying the fitted curves in [16]. Furthermore we thank M. Wadepuhl (Ulm) for proposing and discussing several simulations.

References

[1] Alscher, C. (1995). Numerische Methoden zur Lösung differentiell–algebraischer Gleichungen mit einer Anwendung auf das Hydroskelett. Diploma thesis, University of Bielefeld.

[2] Chapman, G. (1950). On the movement of worms. *J.exp.Biol.* **27**, 29-39.

[3] Chiel, H.J., Crago, P., Mansour, J.M. & Hathi, K. (1992). Biomechanics of a muscular hydrostat: A model of lapping by a reptilian tongue. *Biol.Cybern.* **67**, 403-415.

[4] Ekeberg, Ö. (1993). A combined neuronal and mechanical model of fish swimming. *Biol.Cybern.* **69**, 1-12.

[5] Fauci, L.J. & Peskin, C.S. (1988). A computational model of aquatic animal locomotion. *J.Comp.Phys.* **77**, 85-108.

[6] Fung, Y.C. (1993). Biomechanics: Mechanical properties of living tissues (2nd ed.). Springer–Verlag.

[7] Greenwood, D.T. (1977). Classical dynamics. Prentice Hall.

[8] Jordan, C.E. (1994). Mechanics and dynamics of swimming in the medicinal leech Hirudo medicinalis. Ph.D. thesis, University of Washington.

[9] Kier, W.M. & Smith, K.K. (1985). Tongues, tentacles and trunks: The biomechanics of movement in muscular–hydrostats. *Zool.J.Linn.Soc.* **83**, 307-324.

[10] Kristan, W.B., Stent, G.S. & Ort, C.A. (1974). Neuronal control of swimming in the medicinal leech: I. Dynamics of the swimming rhythm. *J.Comp.Physiol.* **94**, 97-119.

[11] Kristan, W.B., Wittenberg, G., Nusbaum, M.P. & Stern–Tomlinson, W. (1988). Multifunctional interneurons in behavioral circuits of the medicinal leech. *Experientia* **44**, 383-389.

[12] Lubich, C., Nowak, U., Pöhle, U. & Engstler, C. (1992). MEXX – Numerical software for the integration of constrained mechanical multibody systems. Preprint SC 92-12, ZIB.

[13] Mann, K.H., (1962). Leeches (Hirudinea). Their structure, physiology, ecology and embryology. Pergamon Press.

[14] Muller, K.J., Nicholls, J.G. & Stent, G.S. (1981). Neurobiology of the leech. Cold Spring Harbor.

[15] Stern–Tomlinson, W., Nusbaum, M.P., Perez, L.E. & Kristan, W.B. (1986). A kinematic study of crawling behavior in the leech, Hirudo medicinalis. *J.Comp.Physiol.A* **158**, 593-603.

[16] Skierczynski, B.A., Wilson, R.J.A., Kristan, W.B. & Skalak, R. (1996). A model of the hydrostatic skeleton of the leech. *J.theor.Biol.* **181**, 329-342.

[17] Trueman, E.R. (1975). The locomotion of soft–bodied animals. Edward Arnold Limited, London.

[18] Wilson, R.J.A., Skierczynski, B.A., Blackwood, S., Skalak, R. & Kristan, W.B. (1996). Mapping motor neuron activity to overt behaviour in the leech: Passive biomechanical properties of the body wall. *J.Comp.Physiol.* **178**, 637-654.

[19] Wilson, R.J.A., Skierczynski, B.A., Blackwood, S., Skalak, R. & Kristan, W.B. (1996). Mapping motor neuron activity to overt behaviour in the leech: Internal pressures produced during locomotion. *J.Exp.Biol.* **199**, 1415-1428.

[20] Wadepuhl, M. & Beyn, W.–J. (1989). Computer simulation of the hydrostatic skeleton. The physical equivalent, mathematics and application to worm–like forms. *J.theor.Biol.* **136**, 379-402.

[21] Wadepuhl, M., Beyn, W.–J. & Alscher, C. (1997). Stepwise adaptation of a computer model to the leech Hirudo medicinalis L. I. Prediction of muscle forces and pressure. Preprint, University of Bielefeld.

[22] Wadepuhl, M., Beyn, W.–J. & Alscher, C. (1997). Stepwise adaptation of a computer model to the leech Hirudo medicinalis L. II. Effects of geometry, compartmentalization and nonlinear length–tension curves. Preprint, University of Bielefeld.